processes

MDPI

Article

Industrial Implementation of Digital Twin in the Tissue Paper Converting System

Haoliang Cui [1,2], Xiansheng Guo [1], Mohan Wang [3], Dedong Zhang [4,*], Jiwei Zhang [3,5], Yun Zhang [2], Feng Gu [6] and Shaozhang Niu [3]

[1] School of Information and Communication Engineering, University of Electronic Science and Technology of China, Chengdu 610054, China; haoliang.cui@vbooster.cn (H.C.); xsguo@uestc.edu.cn (X.G.)
[2] Southeast Digital Economy Development Institute, Quzhou 324000, China; zhangyun999666@dingtalk.com
[3] School of Computer Science (National Pilot Software Engineering School), Beijing University of Posts and Telecommunications, Beijing 100876, China; wangmohan011004@163.com (M.W.); jwzhang666@bupt.edu.cn (J.Z.); szniu@bupt.edu.cn (S.N.)
[4] China Academy of Railway Sciences Corporation Limited, Beijing 100081, China
[5] Key Laboratory of Interactive Technology and Experience System, Ministry of Culture and Tourism, Beijing University of Posts and Telecommunications, Beijing 100876, China
[6] Department of Computer Science, College of Staten Island, The City University of New York, 2800 Victory Boulevard, Staten Island, NY 10314, USA; feng.gu@csi.cuny.edu
* Correspondence: zhangdedong@rails.cn

Abstract: The tissue paper converting system involves critical stages, including unwinding, embossing, folding, stacking, cutting, and packaging. Despite its maturity, challenges such as production interruptions during roll changes, equipment coordination issues, and unstable packaging speeds persist, affecting overall efficiency. While existing methods like fast roll change mechanisms and automated speed regulation systems have improved individual equipment performance, they fall short in achieving system-wide optimization. This paper proposes a digital-twin-based framework for the tissue paper converting system. High-precision simulation models are developed for key equipment, including the base paper roll stand, folding machine, paper stacker, and packaging machine, enabling real-time system monitoring and prediction. Key performance indicators such as base paper availability, folding speed, stacking status, and packaging progress are effectively predicted, preventing interruptions and reducing downtime. The proposed framework was validated in a real-world application at a Chinese paper manufacturing company. Results show that it increases machine runtime by 3 h per day, improving production efficiency by 15%. This leads to an additional daily output of 35,000 packs, contributing approximately CNY 85,000 in revenue growth. Additionally, the system helps prevent 300 kg of base paper waste daily, saving CNY 600 in manufacturing costs per day.

Keywords: tissue paper; paper converting system; digital twin; simulation; prediction

check for updates

Academic Editor: Maoyin Chen

Received: 11 February 2025
Revised: 19 March 2025
Accepted: 24 March 2025
Published: 26 March 2025

Citation: Cui, H.; Guo, X.; Wang, M.; Zhang, D.; Zhang, J.; Zhang, Y.; Gu, F.; Niu, S. Industrial Implementation of Digital Twin in the Tissue Paper Converting System. *Processes* **2025**, *13*, 986. https://doi.org/10.3390/pr13040986

Copyright: © 2025 by the authors. Licensee MDPI, Basel, Switzerland. This article is an open access article distributed under the terms and conditions of the Creative Commons Attribution (CC BY) license (https://creativecommons.org/licenses/by/4.0/).

1. Introduction

Household paper is an essential daily necessity in modern family life, primarily used for various cleaning purposes [1]. As a fundamental consumer product, household paper offers softness, absorbency, and convenience, meeting consumers' needs for hygiene and comfort [2]. Among household papers such as tissue paper, paper handkerchiefs, wipes, and paper towels, tissue paper is particularly popular due to its single-sheet extraction design, which reduces cross-contact, enhances hygiene, and provides ease of use [3]. As people increasingly emphasize hygiene standards and quality of life, tissue paper has

gradually become a mainstream product in the household paper market, with consumer demand growing rapidly [4].

The tissue paper converting system begins with the base paper roll stand, where the base paper is unwound, divided into layers [5], embossed [6], and folded into paper stacks for single-sheet extraction [7]. After folding, the stacks are stored in the paper stacker, cut to the required lengths, and packaged into individual products [8]. Each step involves critical equipment, such as the roll stand, folding machine, paper stacker, and packaging machine, whose efficient operation is key to system performance. However, several issues persist. The softness of the base paper causes production interruptions and waste during roll changes [9]. Also, the folding machine often lacks coordination with downstream equipment, leading to speed fluctuations and mismatches in paper consumption and production rates. The paper stacker can overload or run out of material under high-intensity conditions, requiring manual intervention. Lastly, instability in the packaging machine's speed can disrupt material supply to the stacker, causing unplanned downtime [10].

To address these challenges, several solutions have been developed. For the base paper roll stand, fast paper roll change mechanisms [11] and residual paper removal devices [12], combined with tension control systems, enable efficient roll changes and minimize waste. To improve coordination between the folding machine and downstream equipment, automatic speed synchronization systems [13] ensure consistent production rhythms, preventing downtime caused by speed fluctuations. The issue of overloading or material shortages in the paper stacker is addressed by using real-time sensor monitoring to detect material status and ensure a stable supply [14]. For the packaging machine, automated speed regulation systems improve synchronization with upstream equipment, reducing downtime from production rate instabilities. While these methods have improved individual equipment performance, further advancements are needed for holistic system optimization.

With the progress of digital transformation, digital twin technologies are being widely used in industries. They allow for real-time tracking of physical systems in a virtual space and help predict equipment performance and product behavior [15]. Recognized as one of the top technology trends by Gartner from 2017 to 2019, digital twins play a key role in driving enterprise transformation and value creation [16]. By integrating real-time data with simulation models, digital twin achieves intelligent perception [17], real-time monitoring [18], dynamic simulation, and process optimization [19]. These capabilities significantly enhance production efficiency, reduce equipment failure risks, and optimize resource allocation [20]. The extensive application of digital twin provides robust technical support and research directions for the intelligent and modernized upgrade of tissue paper converting systems.

Through our factory tests, we find that unplanned downtime caused by key equipment such as the base paper roll stand leads to production interruptions, material waste, and efficiency loss in the tissue paper converting system. Statistical data show that each production line loses 2–3 h daily due to these issues, reducing time utilization by 8–12% and causing significant material waste, with some lines losing up to 300 kg of base paper per day. To address these challenges, this paper integrates mechanistic and empirical models within a digital twin framework to develop a simulation system that predicts potential operational states and efficiency bottlenecks through synchronous and asynchronous simulations [21]. By analyzing extensive simulation data and leveraging industry expertise, this system provides a proactive approach to minimizing downtime risks and optimizing material utilization, enhancing both production stability and economic efficiency.

The main contributions of this paper are as follows: First, we propose a digital-twin-based framework for the tissue paper converting system. High-precision simulation models are developed for key equipment in the tissue paper converting process—namely, the base paper roll stand, folding machine, paper stacker, and packaging machine—accurately reflecting their operational states and roles. Second, based on the simulation models, key performance indicators in the tissue paper converting system are predicted, including base paper availability, folding speed, paper stacking status, and packaging progress. These predictions effectively prevent production interruptions and machine downtime, enhancing production efficiency. Finally, the proposed framework is applied to a paper manufacturing company in China, validating its effectiveness in a real-world production scenario.

2. Related Work

Household paper products, including tissue paper, paper handkerchiefs, wipes, and paper towels, are made from wood, waste paper, or other plant fibers [22] and then converted into various paper products [23]. These paper products play a crucial role in daily life, with each type serving a unique function and purpose. Taking tissue paper as an example, it is a convenient household item widely used in places such as living rooms and dining rooms. Its main features include single-sheet dispensing, which makes it easy to store and carry, as well as good absorbency and softness, providing a comfortable user experience [24]. As market demand diversifies, tissue paper has also incorporated additional functions such as antibacterial properties and fragrance, further enhancing its hygiene and comfort, making it an indispensable daily necessity in modern life [25].

The converting of tissue paper begins with the base paper, which is typically in large roll form [26]. The base paper roll is unwound using a base paper roll stand, ensuring smooth transportation through subsequent equipment. Modern systems typically use motor-driven belts for unwinding the paper, along with tension control systems that adjust the tension based on the tissue paper's characteristics and equipment settings. Next, the paper undergoes embossing, where pressure is applied via engraved rollers to create patterns on the paper [27]. This step not only enhances the aesthetic appeal but also improves the paper's texture and functionality, such as increasing its absorbency and tear resistance. After embossing, the paper moves on to the folding stage, where it is folded into standard sizes and shapes as required, ensuring that each sheet is easy to access and use [28]. Following folding, the paper is precisely cut to ensure uniform size and compliance with packaging requirements. After these steps, the tissue paper enters the final packaging stage, typically using automated packaging machines for sealing [29]. Through this series of processing steps, the base paper is ultimately transformed into convenient tissue paper.

With the rapid advancement of digital technologies, digital twin offers a new approach to optimization in the paper industry. The concept, originally introduced by Michael Grieves as the "information mirroring model", has evolved into a multidisciplinary framework. It combines physical models, sensor data, and historical information to create a virtual representation of physical products throughout their entire life cycle [30]. As early as 2010, NASA applied digital twin for diagnostics and predictive analysis in the aviation sector. Subsequently, the U.S. Air Force utilized it for real-time monitoring and fault prediction in fighter jet maintenance [31]. Siemens also introduced digital twin into manufacturing, significantly improving production quality and efficiency [32]. Although China started exploring digital twin later, interest from academia and industry has grown rapidly. Tao et al. were the first to propose the concept of a digital twin workshop, elaborating on its components and operational principles [33]. Zhuang et al. defined the digital twin as the digital representation of physical entities for simulation and optimization purposes [34],

while Tang et al. emphasized a closed-loop system integrating the entire manufacturing process for analysis and control [35].

In recent years, the concept of digital twin has made significant progress across various fields. Liu et al. proposed an adaptive modeling method based on bionic principles for high-precision monitoring of aerospace components [36]. Dwyer et al. applied digital twin to optimize energy production and scheduling in smart cities [37]. Digital twin has also demonstrated strong application potential in healthcare [38], logistics, and modern agriculture [39], driving innovation and efficiency across industries. Moreover, the integration of digital twin with other digital technologies has brought unprecedented innovation and efficiency improvements to various sectors. In combination with IoT [40], a digital twin can acquire and analyze large volumes of sensor data in real time, enabling advanced monitoring and predictive capabilities for physical equipment and systems. Integration with artificial intelligence (AI) allows digital twin systems to continuously learn and optimize themselves, adapting to different environments and conditions while enhancing their intelligence [41]. When combined with virtual reality (VR) and augmented reality (AR), digital twin offers intuitive visualization and training platforms [42]. The comprehensive application of these digital technologies not only enhances production efficiency and product quality but also serves as a critical engine for digital transformation.

Although digital twin has shown significant potential in various fields, its application in traditional manufacturing, especially in the paper industry, remains insufficient. Most existing research is theoretical, focusing on the advantages of digital twin without addressing its practical implementation in real-world production environments. While digital twin has been successfully applied in sectors like aerospace and smart cities, its adoption in paper manufacturing is still lacking. Challenges in the paper industry, such as raw material diversity, high automation requirements, and reliance on traditional production stability, have delayed the widespread use of digital twin technology.

This paper addresses these gaps by offering a practical application of digital twin in the tissue paper converting process. We have developed and implemented a simulation and prediction system that bridges the gap between theoretical models and real-world application in paper manufacturing. The system has been successfully applied at a well-known paper manufacturing company in Zhejiang, China, leading to significant improvements in production efficiency and resource optimization. This practical implementation demonstrates how digital twin can be effectively used to address the challenges of traditional manufacturing, providing valuable insights into how it can promote more intelligent and efficient industrial practices.

3. Overall Framework of the Tissue Paper Converting Simulation System

As shown in Figure 1, the entire tissue paper converting simulation system is divided into three components: the physical space, the data interaction interface, and the virtual space [43]. The physical space primarily includes the actual equipment and process flows of the tissue paper production line, which covers various stages such as the unwinding of the base paper roll, embossing, folding, cutting, and packaging.

As illustrated in the Figure 2, the tissue paper converting line in the physical space consists of multiple pieces of equipment, including eight base paper roll stands responsible for unwinding the base paper and separating it into bottom, middle, and top layers. The number of base paper roll stands used depends on the number of layers and specifications of the tissue paper being converted. For example, six base paper roll stands are used for three-ply tissue paper, and eight base paper roll stands are used for four-ply tissue paper. During the conversion of three-ply tissue paper, the base paper from stands #1, #2, and #3 are combined, as are the base paper from stands #5, #6, and #7. In the production of four-ply

tissue paper, the base paper from stands #1, #2, #3, and #4 are pressed with the base paper from stands #5, #6, #7, and #8. The converted base paper is then conveyed to two embossing machines. Embossing machine #1 receives the base paper from stands #1, #2, #3, and #4, while embossing machine #2 receives the base paper from stands #5, #6, #7, and #8. In the embossing machines, the paper's direction is determined based on the design of the pattern required by the order, and the layers of base paper are bonded together with adhesive to enhance the paper's aesthetic appeal and functionality. After embossing, the base paper continues to the folding machine, paper stacker, and cutting machine. During folding, the base paper is transversely cut and folded according to the order requirements, forming a "V"-shaped long paper stack, which is then sent to the paper stacker for storage. If equipment failure occurs during this process, the paper stacker effectively ensures the continuity of production, preventing interruptions caused by upstream equipment failure. The stored paper stacks are then processed in the cutting machine, where they are cut into the required length according to the order specifications. Beneath the cutting machine, there are four channels, each connected to a packaging machine; thus, the system is equipped with four packaging machines. Finally, the cut paper stacks are subjected to three-dimensional packaging through the packaging machines, with adhesive film tightly wrapping the stacks to ensure the tissue paper is neat, hygienic, and easy for consumers to use.

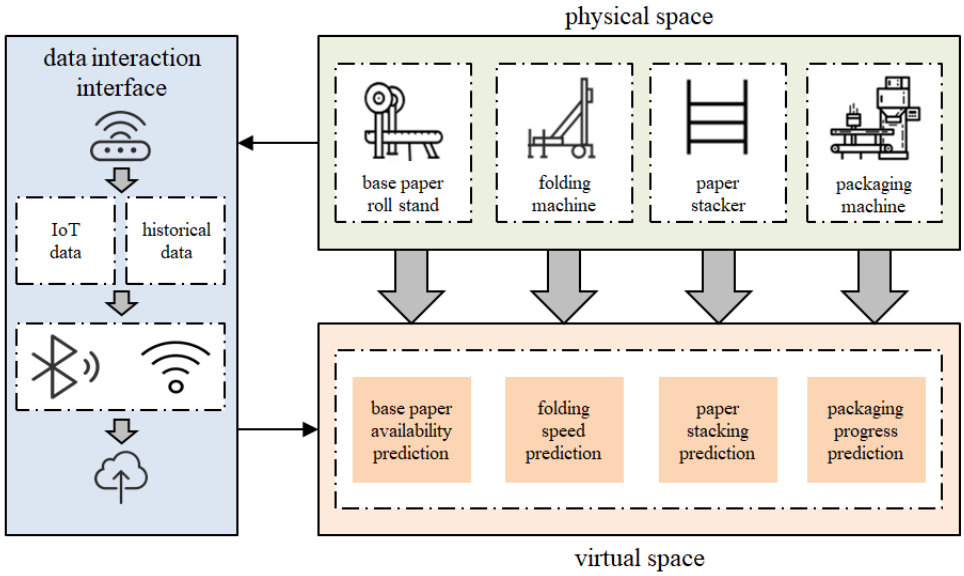


Figure 1. Overall framework of the tissue paper converting simulation system.

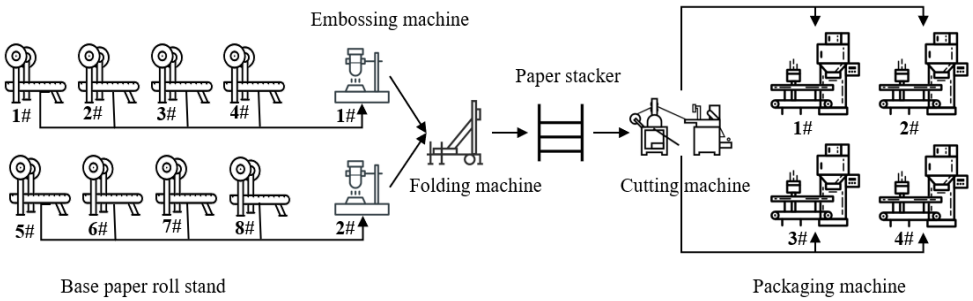


Figure 2. Physical space tissue paper converting process.

The data interaction interface serves as the bridge between the physical space and the virtual space, enabling the effective transmission of various data collected from the physical space to the virtual space. The virtual space, through mathematical modeling and simulation techniques, accurately replicates the operating states and behaviors of the

physical space [44]. In this digital environment, the tissue paper processing system is highly detailed, allowing operators to monitor and analyze the processing flow in real time within the virtual space for optimization and prediction purposes. In the virtual space, we simulate key equipment in the tissue paper processing system, including the base paper roll stand, folding machine, paper stacker, and packaging machine. By predicting the available runtime of the base paper roll stands, the operational speed of the folding machines, the paper storage conditions in the paper stacker, and the packaging progress of the packaging machines, we can effectively prevent unplanned downtime caused by equipment miscoordination, thereby enhancing the time utilization and overall operational efficiency of the production line. This leads to a reduction in material wastage, while improving the stability and economic benefits of the production line. The following chapters will provide a detailed description of the methods for building these four simulation models, as well as the process and results of the model predictions.

4. Simulation Modeling Process for Key Equipment

The simulation modeling process of the tissue paper converting system follows a structured approach, starting with the overall simulation framework and extending to the modeling of key equipment. The system is built based on the operational mechanisms of the entire production line, incorporating event-driven and time-based triggers. To accurately simulate production dynamics, key equipment such as the base paper roll stand, folding machine, paper stacker, and packaging machine are modeled to reflect their operational behaviors and interactions. This allows the system to predict critical production indicators, including base paper availability, folding speed, paper stacking, and packaging progress. The following sections introduce the overall simulation modeling process and specific modeling approaches for each key piece of equipment.

4.1. Overall Simulation Modeling Process

As show in Figure 3, the overall simulation modeling process comprises three key stages: production line construction, simulation execution, and model validation and calibration. This structured approach ensures that the digital-twin-based simulation system accurately represents the actual production line, effectively forecasts critical operational parameters, and undergoes continuous refinement through iterative optimizations. As a result, the system enhances production efficiency and minimizes the risks associated with unplanned downtime.

To construct the simulation model, the system utilizes a knowledge graph of the manufacturing process to replicate the tissue paper converting production line. By integrating simulation models for key equipment, including the base paper roll stand, folding machine, paper stacker, and packaging machine, the system autonomously generates a virtual representation of the entire production workflow. During initialization, the system inputs the real-time operational states of these key components, sets the simulation clock to zero, and generates an event list defining key production events. These initial configurations ensure that all predefined events are executed as planned, providing an accurate simulation of the tissue paper converting process.

During simulation execution, the system takes the real-time state of the production line as its initial condition and advances the simulation clock based on event progression. Events occurring on the base paper roll stand, folding machine, paper stacker, and packaging machine are executed sequentially according to their predefined schedules. Meanwhile, the prediction modules embedded within each key component synchronize with the simulation clock, executing corresponding functions to simulate operational dynamics.

The entire process follows this structured execution, and the simulation concludes when the clock reaches the predefined termination time.

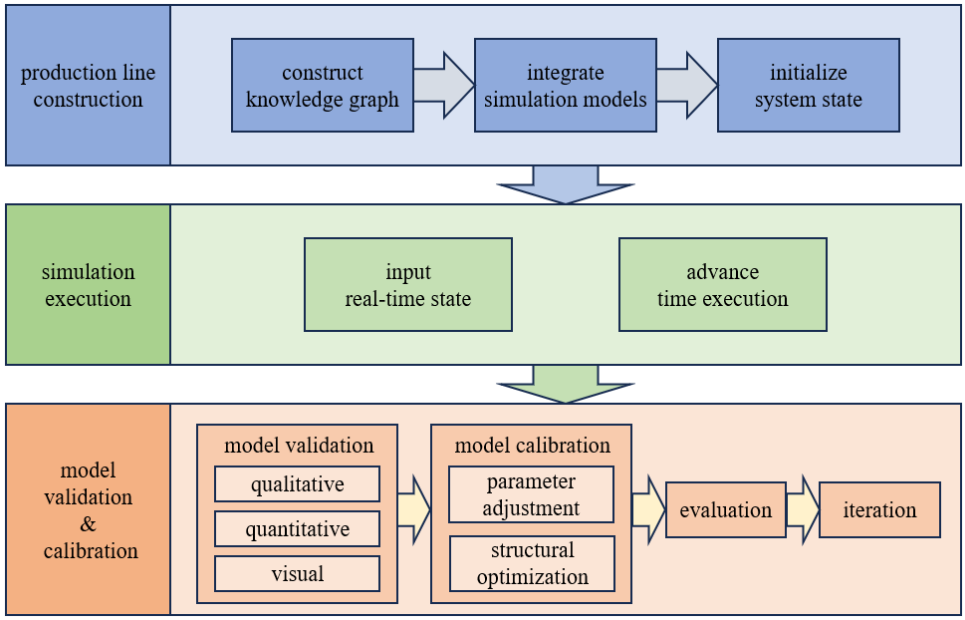


Figure 3. Overall simulation modeling process.

To ensure the accuracy of the simulation model, a comprehensive validation and calibration process is conducted using historical IoT data from the tissue paper converting system. The validation phase systematically compares simulated outputs with actual production data through qualitative, quantitative, and visual analyses. We compare time-series trends of simulated and real-world data to ensure that the model effectively captures fluctuations in key production parameters. If discrepancies are detected, model calibration is performed by adjusting key parameters, refining structural assumptions, and optimizing boundary conditions to align simulation results with real-world performance. The calibration process employs optimization algorithms such as genetic algorithms (GA) and particle swarm optimization (PSO) to minimize the error between the simulation outputs and historical production data. By iteratively searching for the optimal parameter combination, these algorithms enhance the model's predictive capability and improve its generalizability across different production scenarios. This iterative validation and calibration process continues until the model achieves a high level of accuracy and reliability.

4.2. Simulation Modeling Process for the Base Paper Roll Stand

The base paper roll stand primarily stores and supports the base paper to be processed using mechanical devices. Workers typically load the base paper onto the base paper roll stand manually or with mechanical assistance. However, traditional methods for predicting the base paper availability have significant limitations, often leading to unplanned downtime on the production line when the paper runs out, which severely impacts production efficiency. Additionally, workers are required to frequently check the paper's status, increasing labor and time consumption. To address these issues, we have developed an online simulation model for the base paper roll stand to accurately predict the base paper availability. This model can effectively predict the remaining usable time of the base paper based on the remaining meters and outer diameter when the folding machine is operating stably. With this model, production line workers can access real-time information about the base paper availability, enabling more efficient production scheduling and paper management.

As illustrated in Figure 4, the prediction process for base paper availability begins by assessing the operational stability of the folding machine. Based on historical data, the folding machine is considered stable when its speed exceeds a preset threshold and its fluctuation range remains within 1 m per minute. This is determined by comparing the minimum and maximum speed values over a specific preceding period. Once the machine is confirmed to be stable, the prediction process proceeds using two complementary methods. The first method calculates the usable time of the base paper roll based on its remaining length, which is effective when accurate measurements of the outer diameter are unavailable. The second method estimates the usable time based on the roll's current outer diameter, combined with the average tension linear velocity over the same period. These two methods provide flexibility and reliability, ensuring accurate predictions under varying conditions, and the results are used to optimize the production schedule and reduce material waste.

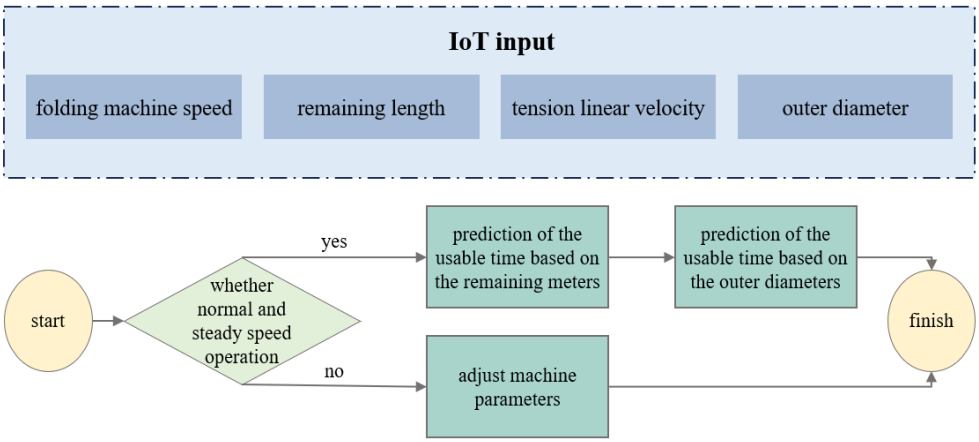


Figure 4. Base paper availability prediction process.

Specifically, we first make a prediction of base paper availability on the base paper roll stand based on the data of the remaining meters of base paper. However, during the use of paper, due to the influence of certain tension, there may be an error between the actual cut length and the remaining meters of the base paper when the folding machine cuts off the base paper. In order to more accurately estimate the service life of base paper, we need to take this bias into account. Therefore, we first use the following calculation formula to obtain the current remaining meters of base paper:

$$L_{current} = L_{initial} - L_{fold} \times s \tag{1}$$

where, $L_{current}$ represents the remaining meters of base paper on the current base paper roll stand, $L_{initial}$ is the initial length of base paper on the base paper roll stand, and L_{fold} represents the length of base paper that has been processed by the subsequent folding machine. In addition, the tension coefficient s is derived by analyzing historical data, reflecting the impact of tension on base paper during the production process, which plays a key role in the consumption rate of base paper.

Next, the base paper availability on the base paper roll stand is estimated by the following formula:

$$T_{available} = \frac{S_{current}}{V_{tension}} \tag{2}$$

$S_{current}$ indicates the remaining meters of base paper on the base paper roll stand, while $V_{tension}$ indicates the average linear speed of tension from the current moment back to a previous period of time. The linear tension speed is the rate of change of the re-

maining meters of base paper, which reflects the actual moving speed of the paper in the production process.

By comprehensively considering these variables and coefficients, the model can more accurately reflect the base paper availability, predict potential shortages or excesses, and minimize downtime and production capacity losses during the manufacturing process.

In actual production, the simulation model for predicting the remaining meters of the base paper is typically calculated based on a manually set total paper length. However, manual settings may sometimes be untimely or incorrect, resulting in less accurate predictions of the remaining meters. To address this, data on the base paper's outer diameter measured by the equipment can be used as a supplementary prediction method. The core of this approach lies in estimating the remaining meters of the base paper based on the rate of reduction in its outer diameter, thereby predicting its usable time. Ideally, the relationship between the change in the outer diameter of base paper and the remaining meters can be approximated by the following formula:

$$V_{paper} \times \rho_{paper} = L_{surplus} \times M_{paper} \tag{3}$$

In this formula, V_{paper}, ρ_{paper}, $L_{surplus}$, and M_{paper} are the volume, density, remaining meters, and mass per unit length of base paper, respectively. If D_{outer} represents the outer diameter of the IoT monitoring base paper on the base paper roll stand, R_{roll} represents the roll radius, and W_{paper} represents the base paper width, then V_{paper} can be calculated by the following formula (Formula (4)):

$$V_{paper} = W_{paper} \times (\pi \times ((D_{outer} + R_{roll}))^2 - \pi \times (R_{roll})^2) \tag{4}$$

According to the above two formulas, we can obtain the derivation formula:

$$\frac{\pi \times W_{paper} \times \rho_{paper}}{M_{paper}} = \frac{L_{surplus}}{((D_{outer} + R_{roll}))^2 - (R_{roll})^2} \tag{5}$$

So, if we write $\frac{\pi \times W_{paper} \times \rho_{paper}}{M_{paper}}$ as the coefficient α and keep α fixed, then we can calculate the remaining meters of base paper given the outer diameter of the base paper. In practice, base paper is often irregular in shape due to factors such as gravity compression, and their density tends to increase as the remaining meters decreases. Therefore, a more accurate method is employed to estimate the remaining meters. First, several evenly spaced remaining meters values are selected, and the corresponding minimum outer diameter values of the base paper are recorded. Using these values, the coefficient α is calculated through a formula, and a coefficient α table is created. Then, the minimum outer diameter r at the current time is identified. Based on the α table, the two outer diameter values r_1 and r_2 adjacent to r, along with their respective coefficients α_1 and α_2, are determined. Assuming a linear relationship between the outer diameter and the coefficient, linear interpolation is used to calculate the coefficient α corresponding to r. Finally, the remaining meters of the base paper is calculated using the obtained α value and the relevant formula:

$$L_{surplus} = \alpha \times ((D_{outer} + R_{roll}))^2 - (R_{roll})^2 \tag{6}$$

By establishing a simulation model for the base paper roll stand, we can accurately predict the base paper availability, effectively preventing unplanned downtime due to paper depletion during production. This predictive approach integrates real-time data on the outer diameter and remaining meters of the base paper, providing dual validation to enhance the accuracy and reliability of predictions. Through this model, production line

operators can proactively monitor base paper consumption, schedule replacements more efficiently, and reduce downtime events, thereby ensuring continuous production flow.

4.3. Simulation Modeling Process for the Folding Machine

When the folding machine operates at a speed that is either too fast or too slow, it creates a chain reaction affecting the material supply and storage levels on both the base base paper roll stand and the paper stacker, potentially leading to production line interruptions. If the folding machine's speed is too fast, the base paper on the base paper roll stand will be consumed at a higher rate, which may cause a shortage of base paper and result in unscheduled downtime. Similarly, an overly rapid folding speed can lead to excessive accumulation of paper reams on the paper stacker, surpassing storage capacity and triggering shutdown alarms. Conversely, if the folding machine's speed is too slow, the production rate of paper reams may fall short of the demand in downstream processes, leading to insufficient stock on the paper stacker and causing delays as subsequent operations wait for material. This imbalance between supply and demand directly impacts the overall efficiency of the production line. Therefore, to maintain continuity and efficiency in production, it is essential to precisely control and adjust the folding machine's operational speed in real time, ensuring alignment with the consumption rate on the base paper roll stand and the accumulation rate on the paper stacker.

To address these issues, we introduced a simulation model for the folding machine. This model predicts the arrival time of each batch of material at the folding machine's inlet and outlet to calculate its actual operating speed. As shown in Figure 5, "NO1" and "NO2" represent the base paper on the base paper roll stand and the paper reams produced by the folding machine, respectively. "B1-X" denotes the six base paper roll stands used for storing base paper, with key parameters including the remaining meters of the base paper, its outer diameter, and the tension line speed. In the model, "P" represents the process of the folding machine producing paper reams at a specific speed, with the main parameter being the folding machine's actual operating speed. "T" indicates the conveying process of transporting folded paper reams to the paper stacker.

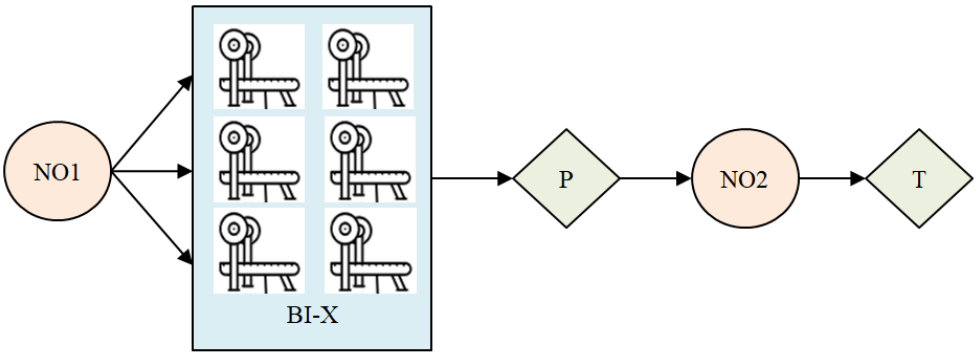


Figure 5. Folding machine section simulation concept diagram.

Assuming the production starts with the first paper ream and ends with the last one, the mathematical model for the number of paper reams produced during this period, N, is expressed as follows:

$$N = \frac{\int_{T_{first}}^{T_{last}} V(t)dt}{C \times \frac{L}{2}} \quad (7)$$

In this formula, T_{first} and T_{last} represent the time point at which the folding machine starts to produce the first paper ream and the last paper ream, respectively, and $V(t)$ represents the running speed of the folding machine under normal operation. Parameters

C and L correspond to the number of draws and the length of single base paper in the product specification of the paper ream.

Assuming each folding transport takes 5 s, the following formula is used to calculate the time when a paper ream is transported to the outlet of the folding machine:

$$T_{out} = T_{in} + 5 \tag{8}$$

where, T_{in} and T_{out} represent the moments when the paper ream arrives at the folding machine's inlets and outlets, respectively.

To further optimize the model, we plan to introduce an appropriate correction factor for the folding machine's operating speed to minimize the discrepancy between the predicted and actual speeds. When both start and end points correspond to changes in the folding machine's inlet, data on the folding machine's input count and operating speed within the same time interval are extracted. Using the data from these two points, the length of the processed base paper is calculated for each. Dividing the former by the latter yields the correction factor β, as shown in the following formula:

$$\beta = \frac{\Delta S \times L \times \frac{C}{2}}{\Delta T \times V_{fold}} \tag{9}$$

where ΔT refers to the start and end time interval of a folding machine running test, ΔS refers to the number of folding machine entering feeds increased by ΔT, L refers to the length of a single paper pack, C refers to the number of draws, and V_{fold} refers to the running speed of the folding machine.

In summary, through precise folding speed adjustments and real-time equipment monitoring, we have not only improved the overall efficiency of the production line but also enhanced the stability and continuity of the production process. This management approach ensures the optimal use of resources during production while also reducing production downtime and capacity losses caused by equipment failures or operational errors.

4.4. Simulation Modeling Process for the Paper Stacker

The paper stacker primarily serves as a temporary storage area for paper reams, using mechanical systems to control the input and output of paper reams on the production line. This ensures synchronized operation between the upstream folding machine and the downstream packaging machine. However, in actual production, the stacker's capacity often struggles to meet the fluctuating demands of production, leading to frequent issues with either paper ream overstock or shortage, both of which affect the stability of the production line. When an excess of paper reams accumulates on the stacker, limited storage space may force the production line to halt the folding machine, causing upstream congestion and reducing overall efficiency. Conversely, if the stacker lacks sufficient paper reams, the downstream packaging machine will experience interruptions, as it runs out of material, leading to further production line delays.

To address these issues, we have achieved independent operation of the paper stacker in a virtual environment by accurately modeling it. By controlling the capacity of the paper reams on the paper stacker, we can effectively prevent production interruptions and ensure the continuous operation of the folding machine and packaging machine. As shown in Figure 6, in the simulation model of the paper stacker, "NO2" and "NO3" represent the paper reams produced by the folding machine and the packages produced by the packaging machine, respectively. "T" represents the process of transferring paper reams by the folding machine, with the main parameter being the transport time for each paper ream. "B2" is the cyclic buffer section of the paper stacker, which connects the folding

machine and the packaging machine, with the main parameter being the storage rate. "B3-X" represents the feeding channels of the four packaging machines, with the main parameter being the operating speed of each packaging machine. By analyzing historical data, we can determine the threshold a, where the paper stacker is full and the folding machine can no longer transfer paper reams, and the threshold b, where the paper stacker is empty and the packaging machine cannot obtain enough paper reams. When the number of paper reams currently stored in B2 is less than threshold a, the paper reams will continue to enter B2. When the stored quantity in B2 is no less than threshold b, the paper reams will be allocated to the B3-X channels based on the available space in each channel. Otherwise, the paper reams will not be able to enter B3-X from B2.

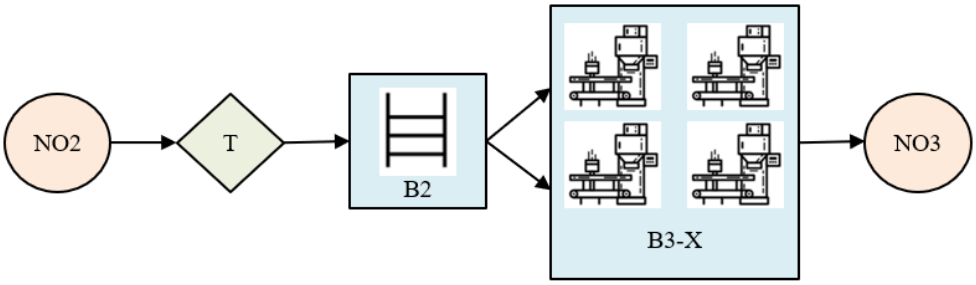


Figure 6. Paper stacker section simulation concept diagram.

As illustrated in Figure 7, the process of predicting the paper storage rate begins by evaluating the operational stability of the folding machine. This is performed by comparing the machine's current running speed with its maximum and minimum values recorded over a preceding time interval. If the current speed falls within this range, the folding machine is considered to be operating normally and stably. The next step is to check whether all sections of the paper stacker contain paper reams. This is verified by analyzing data from the outlet of the folding machine and the inlet of the packaging machine, which indirectly reflects the status of the cyclic buffer section within the paper stacker. By combining this information, we can infer the storage conditions of the cyclic buffer section and accurately predict the paper storage rate. This approach ensures a comprehensive understanding of the paper stacker's operational status, enabling effective predictions under varying conditions.

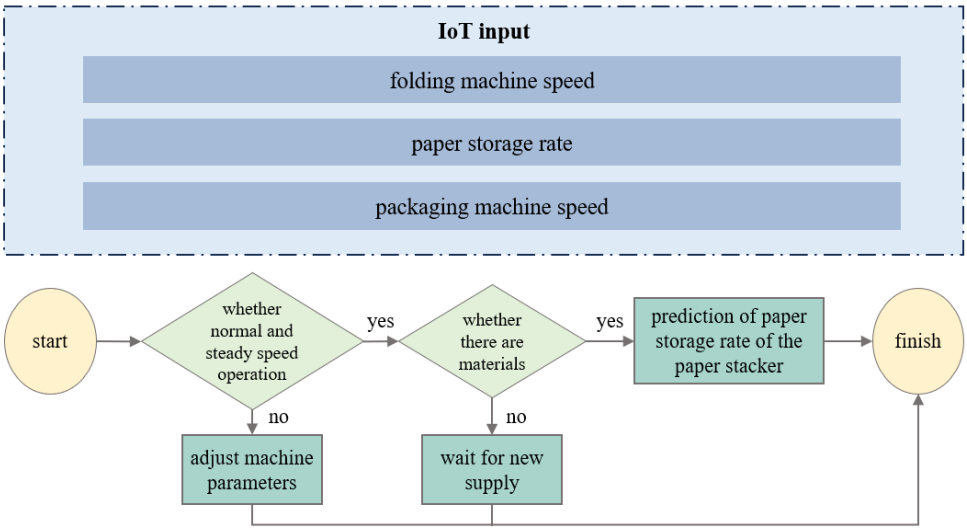


Figure 7. Paper stacking prediction process.

When the predicted storage rate of the paper stacker is too high, it indicates that the stacker is fully loaded and the output from the folding machine exceeds its maximum

capacity. In this case, the folding machine should be paused until sufficient space is freed in the stacker. Conversely, if the storage rate is too low, the number of reams in the stacker is insufficient to meet the requirements of the packaging machine, and the transfer of reams to the packaging machine should be halted. This coordination mechanism effectively balances the production capacity of the folding machine and the packaging machine, ensuring smooth processing of paper reams while minimizing production downtime or resource waste caused by stacker capacity issues.

4.5. Simulation Modeling Process for the Packaging Machine

In the paper industry, packaging machines typically rely on traditional mechanical transmission systems, using gears and belts to perform the cutting, packaging, and boxing of paper reams. Despite the relatively simple process, real-world production faces challenges such as mechanical wear, transmission inefficiencies, and improper equipment adjustments. These issues are especially critical as the operating speed of the packaging machine directly affects the consumption rate of paper reams. When the packaging machine operates too quickly or too slowly, it disrupts the supply rhythm of paper reams from the stacker, potentially leading to unplanned downtime and reduced production line efficiency. To address these issues, we introduced an online simulation model for the packaging machine. By predicting the time each material arrives at the machine's inlet and outlet, the packaging speed can be calculated. Additionally, by predicting the time each material reaches the outlet and the quality checkpoint, the packaging machine's qualification rate can be determined. This monitoring method enables the early identification of potential fault areas on the production line, allowing for preemptive measures to be taken and preventing losses caused by the accumulation of defective products.

As shown in Figure 8, paper reams are conveyed into the packaging machine via a conveyor belt. The packaging machine is responsible for completing multiple processes, including receiving, positioning, and packaging the paper reams in a predefined sequence, transforming them into finished packages. The machine is equipped with a built-in quality inspection module, which automatically ejects any defective packages upon detection. After packaging, the finished packages exit the machine and enter the visual inspection module. This module uses advanced vision technology to inspect each package, identifying defective products for ejection, thereby ensuring product quality. Based on statistical analysis of historical data, the probability of rejecting a package in the quality inspection module is set to 0.0072, while the probability of rejecting a package in the visual inspection module is set to 0.0152.

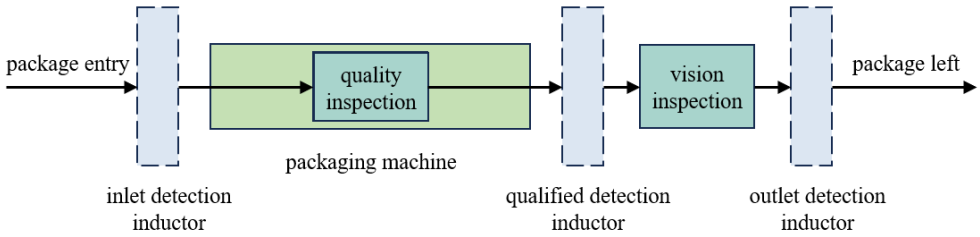


Figure 8. Production diagram of packaging machine section.

The distance from the inlet to the outlet of the packaging machine can be regarded as a special conveyor belt with a length of 2.5 m and a normal operating speed of 0.3788 m per second. During production, a specific model of paper stack is used, with a width of 0.0975 m and a minimum allowable gap of 0 m between reams. As the paper reams move

along the conveyor belt from the inlet to the outlet, the discharge time at the outlet can be calculated based on the known belt speed, using the following formula:

$$T_2 = T_1 + (l_1 + w_1)/v_1 \tag{10}$$

In this formula, T_1 and T_2 represent the times when the paper stack reaches the inlet and exits the outlet, respectively. l_1 denotes the distance between the inlet and the outlet, w_1 indicates the width of the paper stack for the selected product model, and v_1 represents the conveyor speed under normal operating conditions for this section of the production line.

Similarly, the distance from the outlet to the quality checkpoint can also be considered a conveyor section, with a length of 1.7 m and a normal operating speed of 0.4114 m per second. Based on actual product requirements, the length of each package is set to 0.133 m, with a minimum allowable gap of 0 m between packages. The time when a package leaves the quality checkpoint can be calculated using a similar formula:

$$T_4 = T_3 + (l_2 + w_2)/v_2 \tag{11}$$

In this formula, T_3 and T_4 represent the time a specific package reaches the outlet and leaves the quality checkpoint, respectively. l_2 denotes the distance between the outlet and the quality checkpoint, w_2 represents the length of the selected package model, and v_2 indicates the conveyor speed in this section of the production line under normal operating conditions.

Through the predictions made by the above packaging machine simulation model, we can optimize the packaging progress of the packaging machine, promptly identify potential faults, and take measures to minimize economic losses caused by production interruptions and quality issues.

5. Experiments and Results

5.1. Experimental Settings

We applied a digital-twin-based simulation system to the tissue paper converting system of a modern household paper company in Guangdong Province. The company integrates research and development, production, and sales, with a registered capital of over 100 million dollars and nearly 10,000 employees. We deployed simulation models for the paper reel, folding machine, paper stacker, and packaging machine, successfully simulating the real operational status of the tissue paper converting system. By predicting the base paper availability, folding speed, paper stacking, and packaging progress, the system effectively addressed unplanned downtime issues, reduced production costs, and improved production efficiency. Next, we will present the experimental results of each simulation model.

5.2. Prediction of the Base Paper Availability

To validate the effectiveness of the paper reel simulation model, we selected data from periods when the folding machine was operating normally and at a steady speed. Predictions of the base paper availability are made based on both the remaining meters and outer diameters of the base paper, and the results are compared with actual data.

As shown in Figure 9, the chart illustrates the prediction of the remaining meters of base paper on the base paper roll stand. The blue line represents the actual remaining meters recorded by IoT devices, while the orange line represents the predicted remaining meters. It can be observed that the blue and orange lines almost completely overlap, indicating the model's high accuracy. This demonstrates the model's ability to accurately

predict the remaining meters of base paper on the base paper roll stand, providing a solid foundation for subsequent predictions of the base paper roll stand's usable time.

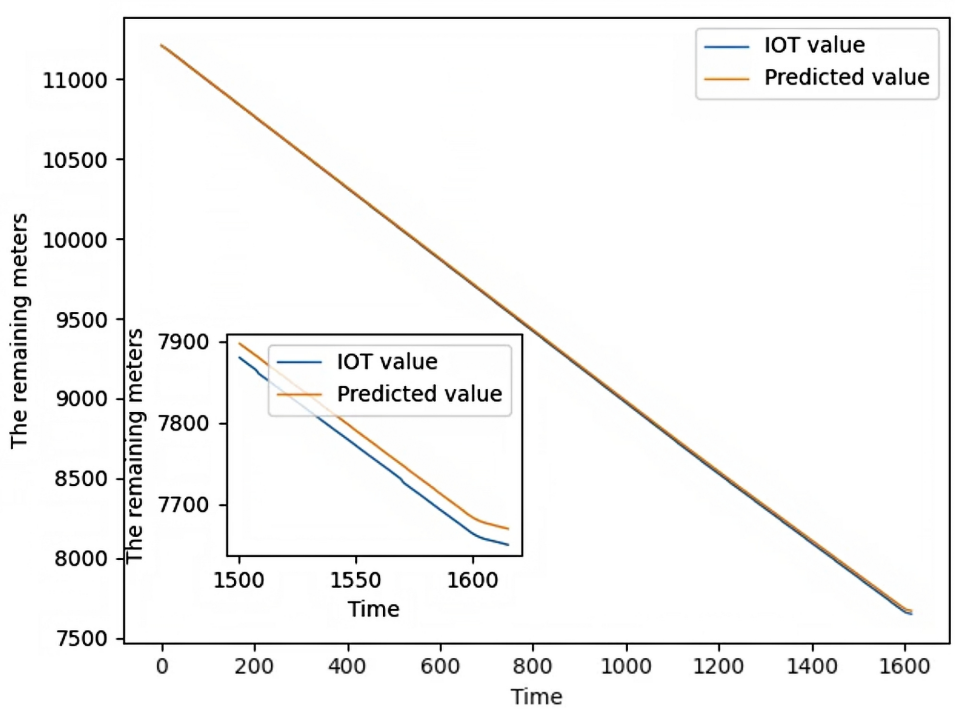


Figure 9. Results of the base paper roll stand remaining meters.

We also created a coefficient α table based on the outer diameter of the base paper, as shown in Table 1, and used it to predict the remaining usable time of the base paper on the base paper roll stand.

Table 1. Table of correction coefficient α.

Base Paper Outside Diameter	Coefficient α
1125	0.0475
942	0.053
794	0.0541
634	0.0556
479	0.0565
352	0.057
96	0.0727

Finally, we validated the effectiveness of the simulation model by combining the remaining meters and outer diameters. Two cases were selected: a decrease from 11,150.84 m to 868.97 m and a decrease from 69,188.04 m to 58,722.36 m. The results are shown in Figures 10 and 11, respectively.

In these two figures, the green line represents the actual recorded values of the base paper availability, the orange line represents the predicted values based on the remaining meters, and the blue line represents the predicted values based on the outer diameter. Although there are differences among the three curves at certain time points, particularly between the orange line and the other two lines, their overall trends are largely consistent. This indicates that our simulation model can accurately predict the base paper availability over a wide range, with predictions based on the outer diameter demonstrating higher accuracy.

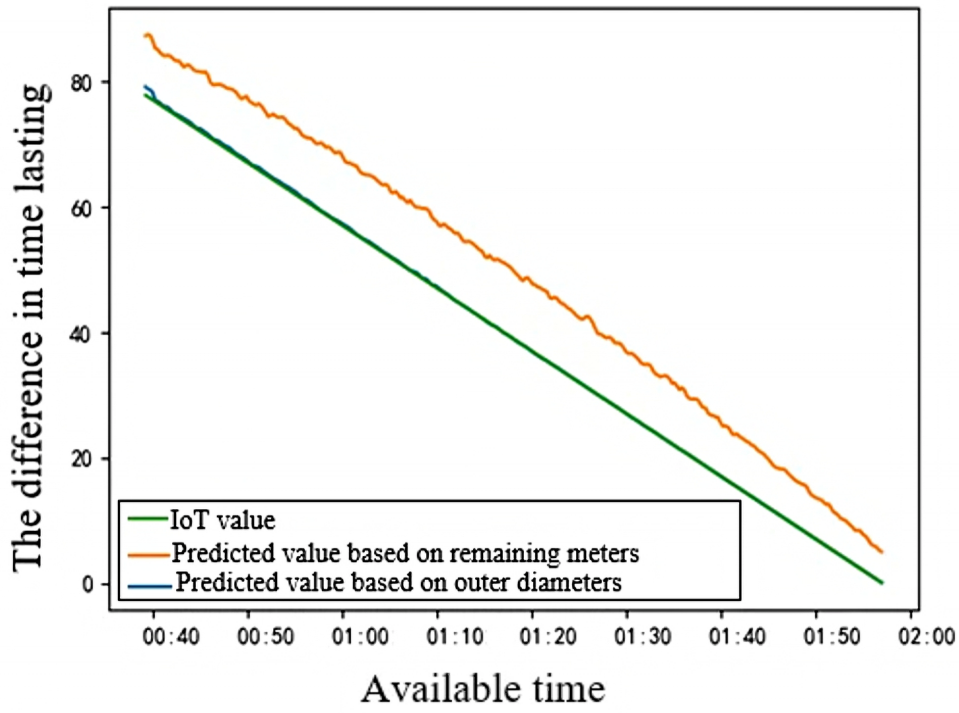


Figure 10. Prediction of usable time of base paper with remaining meters from 11,150.84 to 868.97.

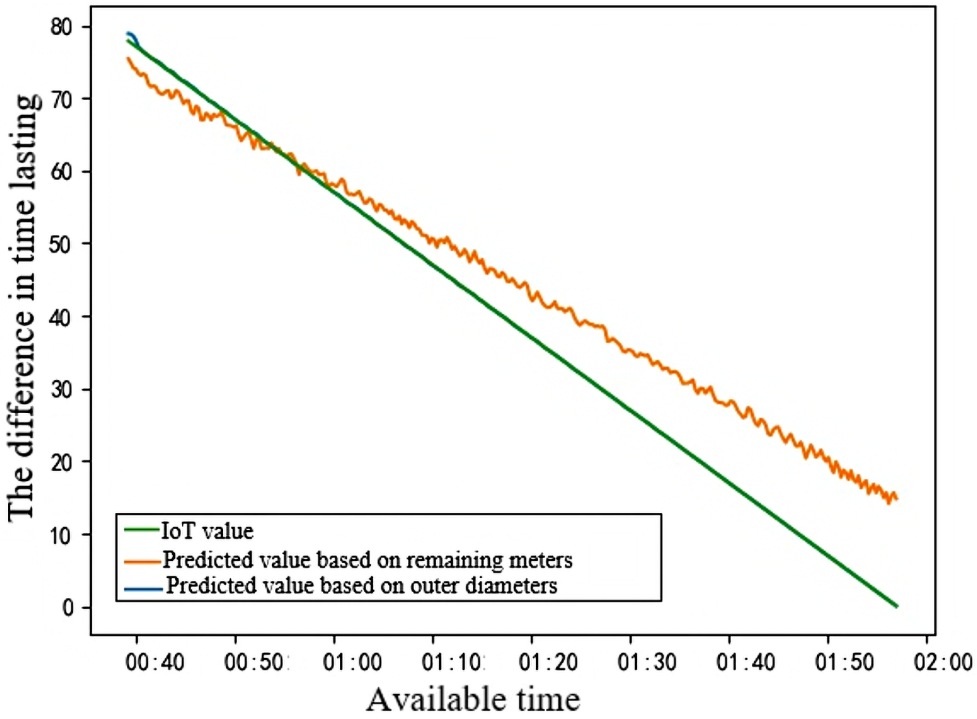


Figure 11. Prediction of usable time of base paper with remaining meters from 69,188.04 to 58,722.36.

5.3. Prediction of the Folding Speed

Based on data from the stable operation phase of the folding machine, we set initial parameters such as product specifications, the remaining meters of base paper on the base paper roll stand, and the number of materials for the folding machine. We developed a folding machine simulation model to predict the times when materials reach the inlet and outlet, calculate the operating speed of the folding machine, and compare the predictions with actual data to evaluate the model's reliability.

As shown in Figure 12, the blue line represents the actual recorded time, while the orange line represents the predicted time. The label "serial number" on the x-axis refers to the sequential number assigned to each material as it enters the machine during the experiment. Initially, the two lines almost overlap, but as the number of materials increases, the gap between them gradually widens. This indicates that the simulation model demonstrates a certain level of accuracy in predicting the time materials reach the inlet, although the error tends to increase as the number of materials grows.

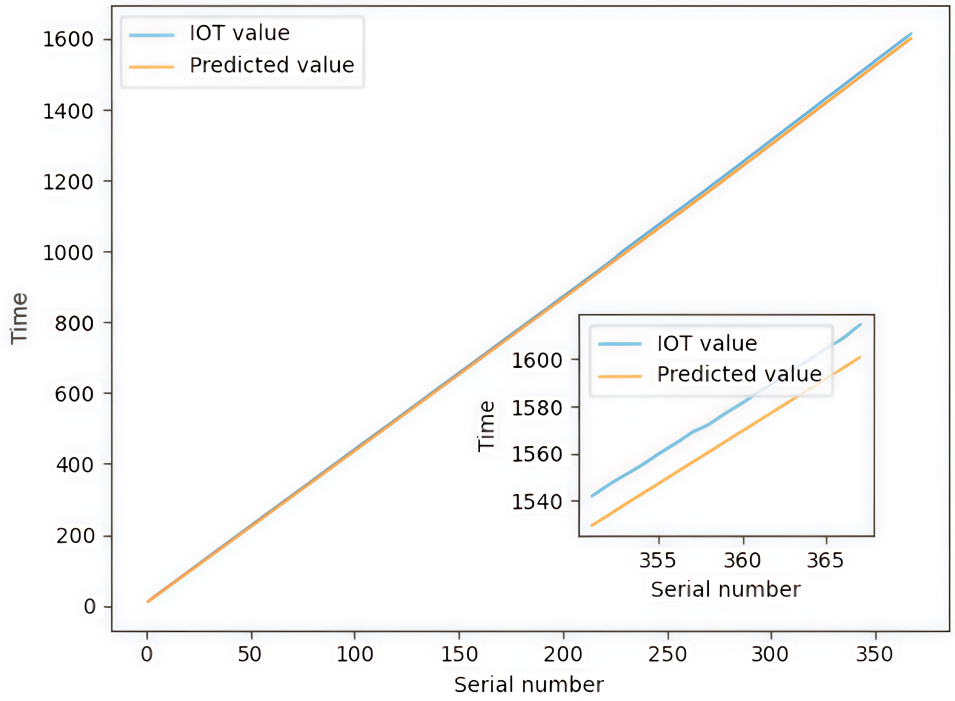


Figure 12. Simulation result diagram of entry number detection inductor.

To enhance the accuracy of the simulation model and more precisely predict the folding speed of the folding machine, we introduced a correction factor of 0.996 to adjust the model. As shown in Figure 13, the orange line and the blue line nearly overlap completely after the adjustment, with errors significantly reduced. These results indicate that the introduction of the correction factor effectively improves the model's accuracy and enables more precise predictions of material arrival times at the folding machine's inlet.

As shown in Figure 14, the blue line represents the actual recorded time, while the orange line represents the predicted time, illustrating the comparison between the predicted and actual recorded time for materials reaching the folding machine's outlet. The label "serial number" on the x-axis refers to the sequential number of each material as it arrives at the folding machine's outlet during the experiment. Initially, the prediction error is extremely small. As the sequential number of materials reaching the outlet increases, the error grows slightly, yet remains generally within an acceptable range.

By predicting the time at which each material reaches the inlet and outlet of the folding machine, we can further calculate its speed. These data not only support workers in preventing interruptions and reducing downtime but also help them more precisely control the operating rhythm of the paper reel and paper stacker. By adjusting the folding speed in real time, workers can effectively minimize unplanned downtime, ensuring the continuity of the production process.

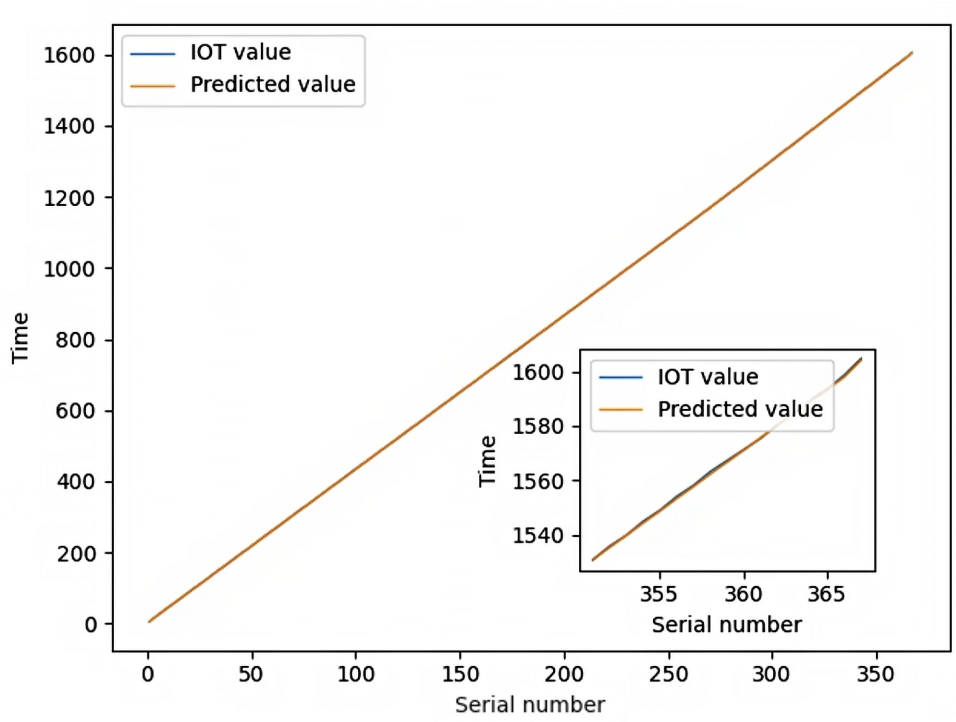


Figure 13. Newly simulation result diagram of entry number detection inductor.

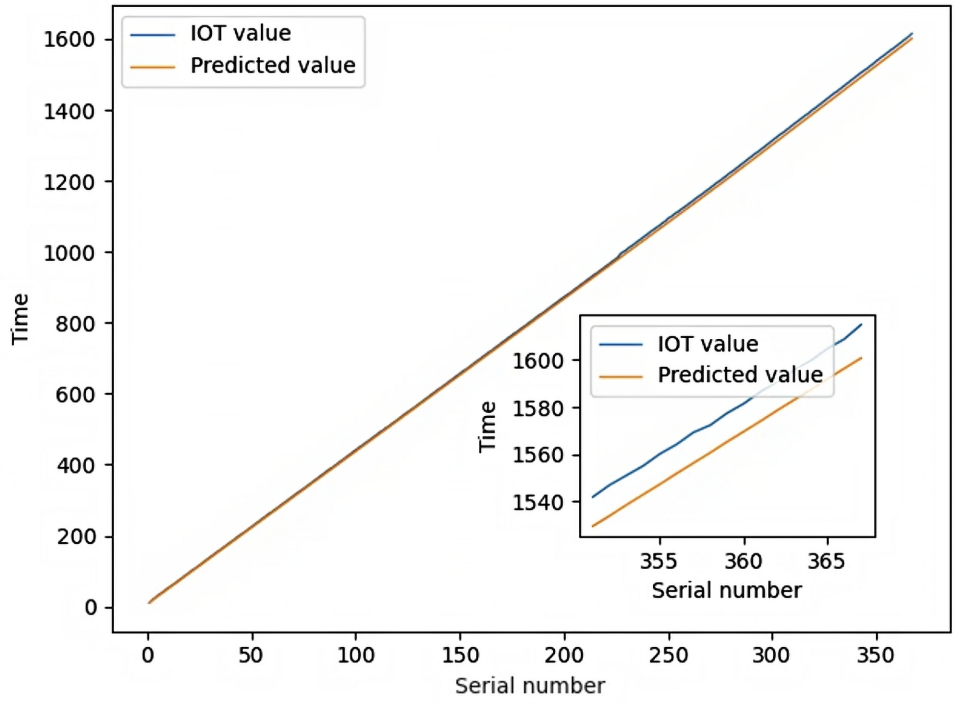


Figure 14. Simulation result diagram of left number detection inductor.

5.4. Prediction of the Paper Stacking

We first developed two simulation models to predict the outlet count of the folding machine and the inlet count of the packaging machine, respectively. Based on these data, we can evaluate whether the cyclic buffer section of the paper stacker is consistently supplied with materials. The specific experimental results are shown in Figures 15 and 16.

In Figure 15, a clear linear relationship can be observed between the predicted data and the actual recorded data, indicating that the simulation model can accurately predict

the output count of the folding machine. Similarly, in Figure 16, the trends of both datasets also exhibit an approximate linear correlation, demonstrating that the simulation model can reliably predict the inlet count of the packaging machine. By analyzing these two sets of predictions, we can assess whether all cyclic sections of the paper stacker, from entry to exit, are supplied with materials.

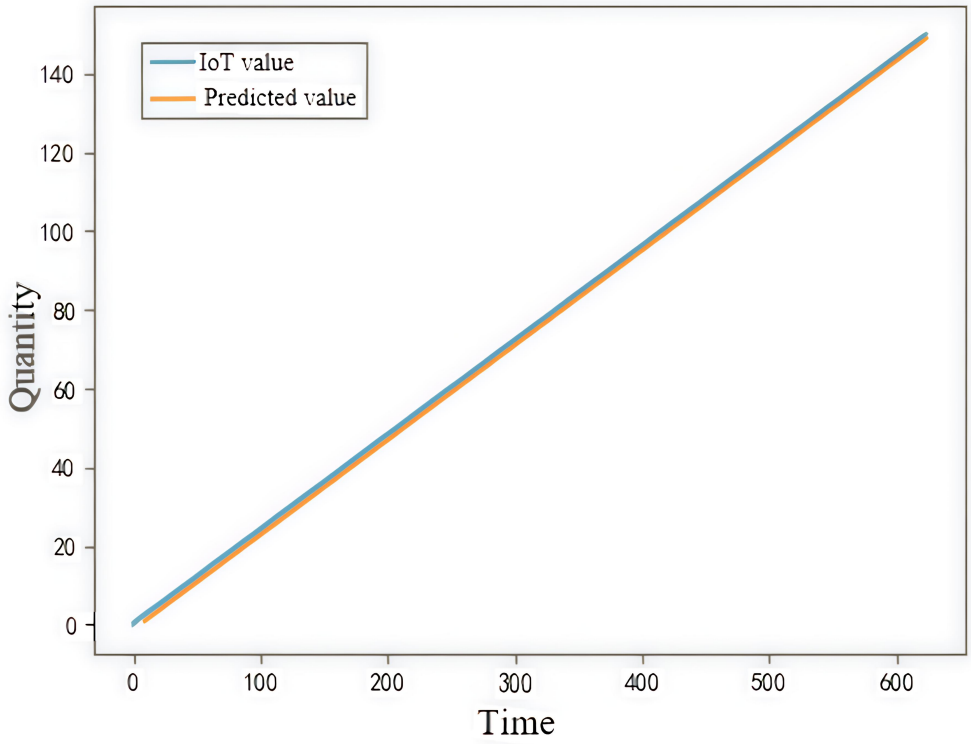


Figure 15. The comparison graph of the number of packages out of the folding machine.

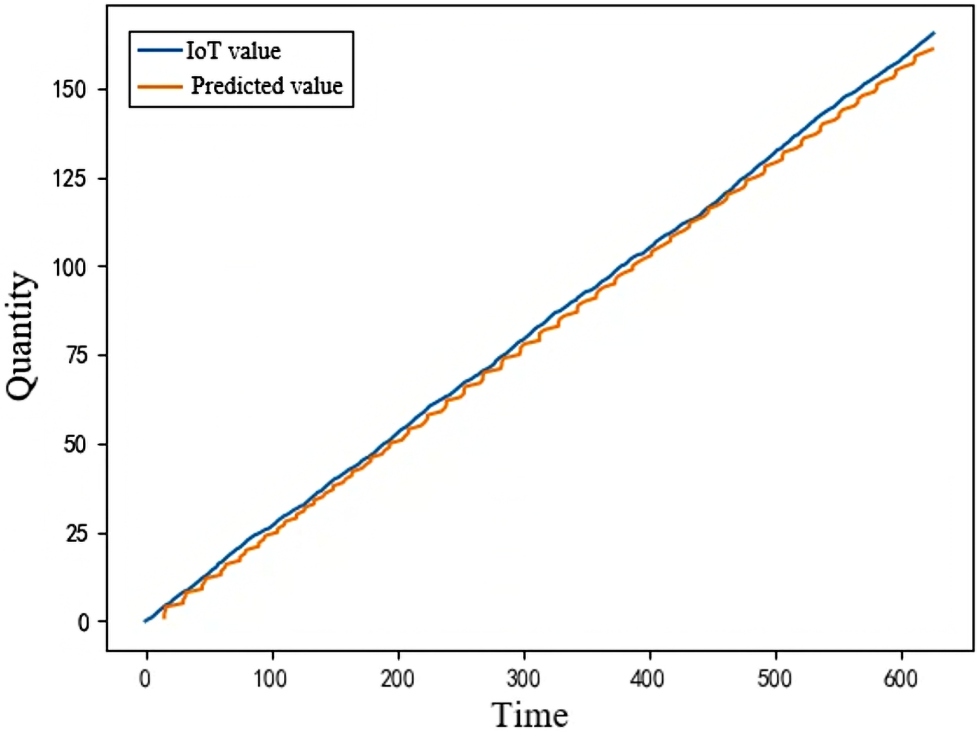


Figure 16. The comparison graph of the effective total number of cuts of the packaging machine.

Consequently, we can proceed to predict the paper storage rate of the paper stacker and compare the predicted data with the actual recorded data, as shown in Figure 17.

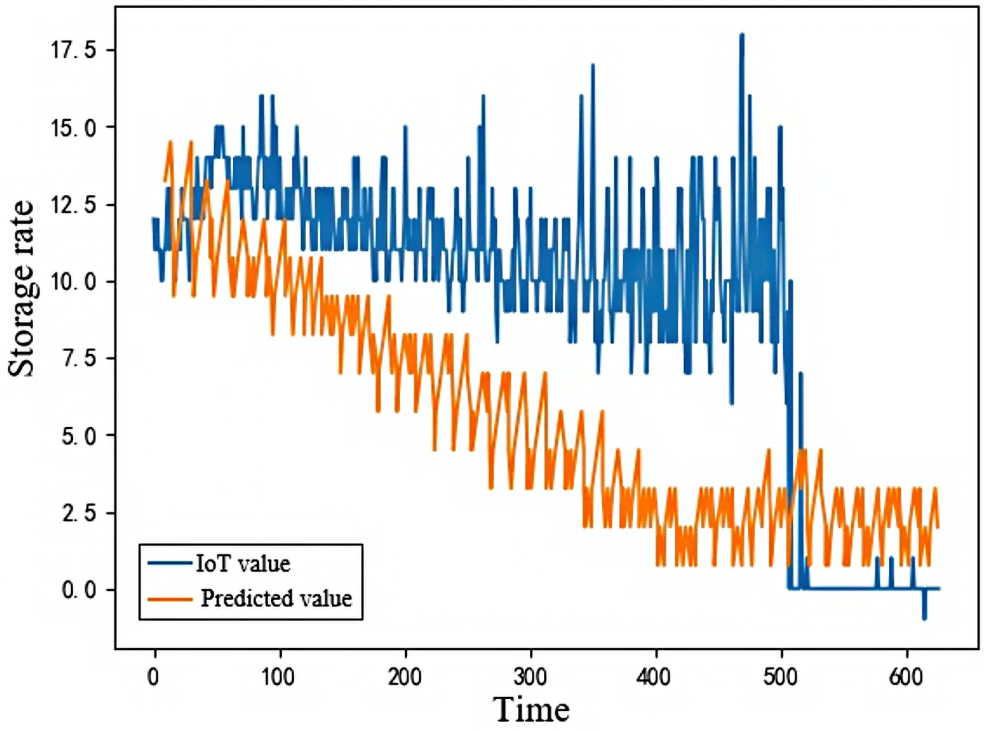


Figure 17. Paper storage rate simulation results.

The orange line in the figure represents the predicted paper stacking rate, while the blue line represents the actual recorded values. Both lines exhibit consistent trends, with no instances of the paper stacker being fully loaded, indicating that the simulation model effectively captures the dynamics of paper stacking. Based on the predictions, potential risks of the stacker reaching full capacity can be identified in advance, allowing timely alerts and parameter adjustment recommendations to be provided to on-site operators. With this optimization, a production line operating 24 h can reduce waste by approximately 90 kg and increase production efficiency by about 5%.

5.5. Prediction of the Packaging Progress

We select the time period during which the packaging machine resumes normal operation after being stopped or in standby mode, to obtain accurate data on the existing materials for predicting the packaging progress. During this period, we are able to accurately record the specific values from each data collection point. Based on these recorded data, we generate the actual input time interval table for the simulation model, which is used as the input parameter for the simulation model, as shown in Table 2.

Through the simulation experiments, we obtain the time points at which each material passes through key stages, and compare the simulation results with the corresponding actual recorded data. The specific results are shown in Tables 3 and 4.

Based on the results in the tables, we can see that the simulation model's performance in predicting the packaging progress of the packaging machine aligns closely with the actual data. Overall, the simulation model shows minimal discrepancies with the actual recorded data in predicting total input volume, outlet count, and qualified count. Additionally, the timing of key events predicted by the model corresponds well with the actual time points, indicating that the model can effectively reflect the operational rhythm of the packaging machine. Although there are some minor deviations, the overall results remain

within an acceptable range, demonstrating the reliability and effectiveness of the simulation model, which can provide strong support for the optimization and adjustment of the production process.

Table 2. Entity input interval table.

Detection Time	Detection Number	Id	Time Interval
00:01:34.681	282,308		
00:01:35.696	282,309	1	1.015
00:01:36.709	282,310	2	1.013
00:01:37.725	282,311	3	1.016
00:01:38.740	282,312	4	1.015
00:01:39.761	282,313	5	1.021
00:01:40.780	282,314	6	1.019
00:01:41.797	282,315	7	1.017
00:01:42.814	282,316	8	1.017
00:01:43.833	282,317	9	1.019
00:01:44.987	282,318	10	1.154
00:01:45.999	282,319	11	1.012
00:01:47.013	282,320	12	1.014
00:01:48.026	282,321	13	1.013
00:01:49.042	282,322	14	1.016
00:01:50.060	282,323	15	1.018
00:01:51.078	282,324	16	1.018
00:01:52.096	282,325	17	1.018

Table 3. Simulation data sheet of packaging machine section.

Data Sources	Actual Data	Simulation Data
Total input	5502	5502
Outlet number	5413	5456
Qualified number	5360	5378

Table 4. Simulation time sheet of packaging machine section.

Data Sources	Actual Time	Simulation Time
Last package input	4844.789	4844.789
Outlet detection	4851.902	4856.1
Qualified detection	4851.902	4856.1
Average for each package	\	11.315

5.6. Production Efficiency and Cost

With the assistance of the tissue paper converting simulation system, overall production efficiency has been significantly improved, while raw paper waste has been effectively controlled, resulting in higher economic benefits. Specifically, the system has increased daily equipment operating time by 3 h, leading to a 15% improvement in production efficiency. As a result, daily output has risen by 35,000 packs, generating an additional CNY 85,000 in daily revenue. This translates to approximately CNY 75,000 in monthly revenue growth per production line and a potential annual revenue increase of CNY 750,000.

Moreover, through system simulation and adjustments, it is possible to reduce 20 downtime events, significantly decreasing raw paper waste. On average, 300 kg of raw paper loss is avoided daily, saving approximately CNY 600 in manufacturing costs per day. This translates to an annual cost reduction of CNY 180,000 per production line. These results highlight the importance of predictive analytics in production management,

demonstrating that digital-twin-based optimization can not only enhance efficiency but also contribute to cost savings and sustainable manufacturing.

6. Discussion

This paper proposes a simulation system for tissue paper processing and establishes four simulation models based on key equipment. The system was validated using a real-world tissue paper production line from a Chinese paper manufacturing company, demonstrating that the digital twin framework can improve production line utilization and reduce unplanned downtime. Although the case study verifies the feasibility of the proposed model, challenges may arise when applying it to different enterprises. For instance, variations in equipment configurations, process parameters, and production environments across different manufacturers may affect the system's adaptability. Additionally, factors such as the age of the equipment, production management practices, and the skill levels of technical personnel may influence the applicability of the model. To enhance its scalability across different tissue paper processing lines, future research will focus on modular system design to improve flexibility and adaptability. Moreover, efforts will be made to integrate the system with traditional production management systems to enable more efficient collaborative optimization.

Data accuracy is crucial for the digital twin model, but sensor noise and missing data are inevitable in real production. The current model mitigates some data errors by implementing threshold-based filtering, historical data analysis, and linear interpolation techniques. However, these methods have limitations, especially in complex production scenarios where data anomalies may lead to misjudgments or simulation deviations. Future work will incorporate anomaly detection and data-cleaning algorithms to enhance robustness. Additionally, the digital twin model relies on real-time data input, which may pose risks related to cyberattacks or data breaches. To address these concerns, we plan to integrate data encryption, access control mechanisms, and blockchain technology into the system to enhance data security and prevent unauthorized access or tampering. Furthermore, establishing data backup and anomaly detection mechanisms will ensure that the system can quickly recover from security threats, maintaining the stable operation of the digital twin system.

While this study focuses on production efficiency optimization, the environmental impact and sustainability of digital twin technology should not be overlooked. Deploying a digital twin system requires installing sensors and utilizing computational resources, which may contribute to resource consumption and carbon emissions. However, in the long run, this technology can optimize industrial processes, reduce raw material waste, and lower energy consumption, thereby decreasing pollutant emissions. Future research will further assess the environmental impact of digital twins and explore strategies for enhancing sustainability.

7. Conclusions

Based on digital twin technology, we propose a comprehensive framework for a tissue paper converting simulation system. By integrating mechanistic and empirical models, the system simulates key equipment operations in the tissue paper converting process, such as the base paper roll stand, folding machine, paper stacker, and packaging machine. This allows for the prediction of critical performance indicators such as base paper availability, folding speed, stacking status, and packaging progress. This research contributes to the application of digital twin technology in industry, particularly in traditional manufacturing sectors. Furthermore, due to the similarities in the processing of tissue paper, paper

handkerchiefs, paper rolls, and other household paper products, this study can be extended to other paper processing systems in the future.

Meanwhile, we implement the digital-twin-based tissue paper converting simulation system framework at a well-known paper manufacturing company in Guangdong Province, China. The results showed that our model accurately predicted key performance indicators, with deviations controlled within 5%. Through system optimization, production efficiency increased by 15%, leading to higher daily output and an annual revenue increase of approximately CNY 750,000 per production line. Additionally, downtime events were significantly reduced, lowering raw paper waste and saving around CNY 180,000 in manufacturing costs annually. These findings demonstrate the practical value of digital twin technology in real-world manufacturing, bridging the gap between theoretical research and industrial application.

In summary, the proposed digital-twin-based tissue paper converting simulation system provides a solid foundation for improving production efficiency and resource optimization in the paper industry. By integrating real-time data with simulation models, the system offers valuable insights into the performance of critical equipment, thereby supporting better decision-making and process optimization. The successful implementation of this system in a well-established paper manufacturing company has demonstrated its practical applicability, with measurable improvements in production efficiency and cost reduction.

Looking ahead, this research lays the groundwork for expanding digital twin applications to other paper processing systems, such as the converting of paper handkerchiefs, paper rolls, and other household paper products. Furthermore, the approach can be adapted and extended to other traditional manufacturing sectors, helping drive the digital transformation of industries that have relied on conventional processes. The continued evolution and integration of digital twin technology, combined with IoT and AI, will open up new opportunities for optimizing production lines, enhancing product quality, and supporting sustainable manufacturing practices across diverse sectors.

Author Contributions: Software, H.C.; methodology, X.G.; writing—original draft preparation, M.W.; validation, D.Z. and Y.Z.; writing—review and editing, J.Z. and F.G.; supervision, S.N. All authors have read and agreed to the published version of the manuscript.

Funding: This work is supported by the National Natural Science Foundation of China under Grant (No. 62171086).

Data Availability Statement: The data and code used in the experimental section of this study are tied to the proprietary operations of a related company and contain sensitive commercial information. Due to the confidentiality agreements in place, we are unable to share these materials publicly.

Acknowledgments: The authors express their gratitude to the Southeast Digital Economy Development Institute for its technical assistance and to the National Natural Science Foundation of China for funding this research.

Conflicts of Interest: Author Dedong Zhang was employed by the company China Academy of Railway Sciences Corporation Limited. The remaining authors declare that the research was conducted in the absence of any commercial or financial relationships that could be construed as a potential conflict of interest. The company had no role in the design of the study; in the collection, analyses, or interpretation of data; in the writing of the manuscript, or in the decision to publish the results.

References

1. Peng, Y.Y.; Chen, R.Q.; Chen, C.X.; Wu, S.B. Thoughts and suggestions on the quality and safety of household paper in China. *China Pulp Pap.* **2012**, *9*, 4.
2. Chang, C.H.; Yu, S.T.; Perng, Y.S. Effects of furnish and refining on properties of household paper. *Cellul. Chem. Technol.* **2018**, *52*, 433–440.
3. Li, R.F. Classification standards for household paper. *Sichuan Pap.* **1994**, *1*, 4.
4. Bunyawairot, D. *An Analysis of Consumer Behavior on Store and National Brands: An Empirical Case from Toilet Tissue Paper* ; Technical Report; Thammasat University: Bangkok, Thailand, 2011.
5. Vieira, J.C.; Fiadeiro, P.T.; Costa, A.P. Converting operations impact on tissue paper product properties—A review. *BioResources* **2023**, *18*, 2303. [CrossRef]
6. Morais, F.P.; Vieira, J.C.; Mendes, A.O.; Carta, A.M.; Costa, A.P.; Fiadeiro, P.T.; Curto, J.M.; Amaral, M.E. Characterization of absorbency properties on tissue paper materials with and without "deco" and "micro" embossing patterns. *Cellulose* **2022**, *29*, 541–555. [CrossRef]
7. Galli, E. *Introduction to Process and Properties of Tissue Paper*; The Navigator Company: Lisbon, Portugal, 2022.
8. Xiong, Q.; Hu, W.J. A Tissue Paper Packaging Adhesive Machine. Patent CN202222379663.1, 21 February 2023
9. Pejic, D. *Identifying and Reducing Converting Paper Waste A Case Study at SCA's Paper Mill in Lilla Edet*; Technical Report; Chalmers University of Technology: Göteborg, Sweden, 2016.
10. Teksan, Z.M. Integrated Production Planning, Shift Planning, and Detailed Scheduling in a Tissue Paper Manufacturer. Master's Thesis, Boğaziçi University, Beşiktaş, Turkey, 2011.
11. Tang, Z.L.; Li, J.H.; Liang, X.Y.; Feng, G.C. A New Rapid Paper Changing Device for a Paper Feeder. Patent CN201610646027.7, 4 January 2017.
12. Zhao, Q.; Jiang, C.J. Fragmentary Paper Unloading Device for Base Paper Roll Stand. Patent CN201620854108.1U, 4 January 2017.
13. Datta, P.; Mohi, G.K.; Chander, J. Automatic paper folding machine WD-298A desktop paper folder office equipment. *J. Lab. Physicians* **2018**, *10*, 6.
14. Yang, T.; Mativetsky, J.M. Based mechanical sensors enabled by folding and stacking. *ACS Appl. Mater. Interfaces* **2019**, *11*, 26339–26345. [CrossRef]
15. Rasheed, A.; San, O.; Kvamsdal, T. Digital twin: Values, challenges, and enablers from a modeling perspective. *IEEE Access* **2020**, *8*, 21980–22012. [CrossRef]
16. Gao, L.B.; Lü, Z.Y.; Suo, H.S.; Liu, X.Y. Current status and development trend of petrochemical process simulation software. *Chem. Eng. Prog.* **2021**, *40*, 1–14.
17. Zhou, G.; Zhang, C.; Li, Z.; Ding, K.; Wang, C. Knowledge-driven digital twin manufacturing cell towards intelligent manufacturing. *Int. J. Prod. Res.* **2020**, *58*, 1034–1051. [CrossRef]
18. Pan, Y.H.; Qu, T.; Wu, N.Q.; Khalgui, M.; Huang, G.Q. Digital twin-based real-time production logistics synchronization system in a multi-level computing architecture. *J. Manuf. Syst.* **2021**, *58*, 246–260. [CrossRef]
19. Ma, J.; Chen, H.; Zhang, Y.; Guo, H.; Ren, Y. A digital twin-driven production management system for production workshop. *Int. J. Adv. Manuf. Technol.* **2020**, *110*, 1385–1397.
20. Zhuang, C.; Liu, J.; Xiong, H. Digital twin-based smart production management and control framework for the complex product assembly shop-floor. *Int. J. Adv. Manuf. Technol.* **2018**, *96*, 1149–1163.
21. Minerva, R.; Lee, G.M.; Crespi, N. Digital twin in the IoT context: A survey on technical features, scenarios, and architectural models. *Proc. IEEE* **2020**, *108*, 1785–1824.
22. Bajpai, P.; Bajpai, P. Brief description of the pulp and papermaking process. In *Biotechnology for Pulp and Paper Processing*; Springer: Berlin/Heidelberg, Germany, 2018; pp. 9–26.
23. Zhang, Z.P.; Dong, K.B.; Li, C.X.; An, X.Y.; Cao, H.B.; Lu, B.; Liu, H.B. Factors affecting the absorbency properties of household paper. *China Pulp Pap.* **2022**, *41*, 89–94.
24. Sa, J.; Li, Z.; Yang, Q.; Chen, X. Packaging defect detection system based on machine vision and deep learning. In Proceedings of the 2020 5th International Conference on Computer and Communication Systems, Shanghai, China, 15–18 May 2020.
25. Liu, G.Y. A Softening and Fragrance-Enhancing Device for Tissue Paper Processing. Patent CN202121994531.9, 11 March 2022.
26. Chen, L.Y. Research and application of the base paper management system in household paper enterprises. *Pap. Pap. Mak.* **2017**, *36*, 5.
27. Vieira, J.C.; Mendes, A.D.O.; Ribeiro, M.L.; Vieira, A.C.; Carta, A.M.; Fiadeiro, P.T.; Costa, A.P. Embossing lines and dots geometry effect on the key tissue paper properties with finite element method analysis. *Polymers* **2022**, *14*, 3448. [CrossRef]
28. Jin, H.Y.; Leng, Q. Tissue paper folding machine with lamination (kitchen towel). *World J. Gastroenterol. WJG* **2015**, *21*, 623. [CrossRef]
29. Coutinho, J.P.; Reis, M.S.; Neves, D.F.M.G.; Bernardo, F.P. Robust optimization and data-driven modeling of tissue paper packing considering cargo deformation. *Comput. Ind. Eng.* **2023**, *175*, 108898. [CrossRef]

30. Parker, D.H. Review of the US patent literature on digital twins and possible applications for coordinate metrology. *Mach. Des.* **2002**, *1*, 2.
31. Glaessgen, E.; Stargel, D. The digital twin paradigm for future NASA and US Air Force vehicles. In Proceedings of the 53rd Structures, Structural Dynamics and Materials Conference (SDM), Honolulu, HI, USA, 23–26 April 2012; p. 1818.
32. Tao, F.; Zhang, H.; Liu, A.; Nee, A.Y. Digital twin in industry: State-of-the-art. *IEEE Trans. Ind. Inform.* **2018**, *15*, 2405–2415.
33. Tao, F.; Zhang, M.; Cheng, J.; Qi, Q. Digital twin workshop—A new model for future workshop operation. *Comput. Integr. Manuf. Syst.* **2017**, *23*, 1–9.
34. Zhuang, C.B.; Liu, J.H.; Xiong, H.; Ding, X.Y.; Liu, S.L.; Weng, G. Connotation, architecture, and development trend of product digital twin. *Comput. Integr. Manuf. Syst.* **2017**, *23*, 753.
35. Tang, T.; Lin, T.; Jie, W.; Ming, C. Digitalization is the only way to intelligent manufacturing—Interpretation of The Road to Intelligent Manufacturing: Digital Factory. *China Mech. Eng.* **2018**, *29*, 366–377.
36. Liu, S.; Bao, J.; Lu, Y.; Li, J.; Lu, S.; Sun, X. Digital twin modeling method based on biomimicry for machining aerospace components. *J. Manuf. Syst.* **2021**, *58*, 180–195.
37. O'Dwyer, E.; Pan, I.; Charlesworth, R.; Butler, S.; Shah, N. Integration of an energy management tool and digital twin for coordination and control of multi-vector smart energy systems. *Sustain. Cities Soc.* **2020**, *62*, 102412.
38. Sarp, S.; Kuzlu, M.; Zhao, Y.; Gueler, O. Digital twin in healthcare: A study for chronic wound management. *IEEE J. Biomed. Health Inform.* **2023**, *27*, 5634–5643.
39. Ghandar, A.; Ahmed, A.; Zulfiqar, S.; Hua, Z.; Hanai, M.; Theodoropoulos, G. A decision support system for urban agriculture using digital twin: A case study with aquaponics. *IEEE Access* **2021**, *9*, 35691–35708.
40. Zhao, Z.; Shen, L.; Yang, C.; Wu, W.; Zhang, M.; Huang, G.Q. IoT and digital twin-enabled smart tracking for safety management. *Comput. Oper. Res.* **2021**, *128*, 105183. [CrossRef]
41. Groshev, M.; Guimaraes, C.; Martín-Pérez, J.; de la Oliva, A. Toward intelligent cyber-physical systems: Digital twin meets artificial intelligence. *IEEE Commun. Mag.* **2021**, *59*, 14–20. [CrossRef]
42. Li, C.; Zheng, P.; Li, S.; Pang, Y.; Lee, C.K. AR-assisted digital twin-enabled robot collaborative manufacturing system with human-in-the-loop. *Robot. Comput.-Integr. Manuf.* **2022**, *76*, 102321. [CrossRef]
43. Grieves, M. *Virtually Perfect: Driving Innovative and Lean Products through Product Lifecycle Management*; Space Coast Press: Cocoa Beach, FL, USA, 2011.
44. Liu, M.; Fang, S.; Dong, H.; Xu, C. Review of digital twin about concepts, technologies, and industrial applications. *J. Manuf. Syst.* **2021**, *58*, 346–361. [CrossRef]

Disclaimer/Publisher's Note: The statements, opinions and data contained in all publications are solely those of the individual author(s) and contributor(s) and not of MDPI and/or the editor(s). MDPI and/or the editor(s) disclaim responsibility for any injury to people or property resulting from any ideas, methods, instructions or products referred to in the content.